Journal of Physiology (1990), **425**, *pp.* 347–367
With 8 figures
Printed in Great Britain

FAST GATING KINETICS OF THE SLOW Ca^{2+} CURRENT IN CUT SKELETAL MUSCLE FIBRES OF THE FROG

BY D. FELDMEYER, W. MELZER, B. POHL AND P. ZÖLLNER

From the Department of Cell Physiology, Ruhr-University Bochum, ND-4, D-4630 Bochum, FRG

(*Received 4 September 1989*)

SUMMARY

1. Calcium currents and intramembrane charge movements were measured in cut twitch muscle fibres of the frog and the time course of activation of the current was studied using various conditioning pulse protocols.

2. When a conditioning activation was produced by a depolarizing pulse which ended before inactivation occurred, a subsequent depolarization led to a faster onset of activation, indicating that the system had not completely returned to the initial state during the interval between the two pulses.

3. The interval between conditioning and test pulse was varied at different subthreshold potentials to study the time course of restoring the steady-state conditions. Complete restoration required a waiting period of about 1 min at the holding potential of −80 mV due to a very slow process but partial recovery was reached within 100 ms. This initial recovery process was strongly voltage dependent and became considerably slower when the interval potential approached the threshold for current activation.

4. Stepping to a roughly 10 mV subthreshold potential without applying a conditioning activation caused no change in the time course of the current produced by a subsequent test depolarization. Depolarizing just to the current threshold caused a slowly progressing acceleration of test current activation.

5. The peak current–voltage relation in the fast gating regime caused by a conditioning activation coincided with the current–voltage relation measured under steady-state conditions, indicating not that a new channel population had become activated but that the same channels showed a different gating behaviour.

6. Intramembrane charge movements measured in 2 mM-Cd^{2+} and tested at potentials between −40 and +40 mV showed negligible changes when preceded by a strong depolarization.

7. We discuss several possible models which can explain the fact that the current is speeded up by a conditioning activation while the charge movements remain unchanged. It is possible that the fast voltage-dependent transition which becomes visible after conditioning pulses reflects a rapid conformational change of the Ca^{2+} channel molecule which also occurs during its normal gating mode but remains undetectable in terms of conductance. In view of the hypothesis that the Ca^{2+} channel molecule forms a voltage sensor for excitation–contraction coupling this fast

MS 7918

transition could be coupled to the control of Ca^{2+} release from the sarcoplasmic reticulum.

INTRODUCTION

The major Ca^{2+} current in adult vertebrate skeletal muscle is a component with the pharmacological sensitivity of L-type currents, but showing extraordinarily slow voltage-dependent activation (Sanchez & Stefani, 1983). The protein exhibiting binding sites for Ca^{2+} channel antagonists, often simply called the dihydropyridine (DHP) receptor, has also been linked, in skeletal muscle, to the process of excitation–contraction (EC) coupling (Rios & Brum, 1987; Tanabe, Takeshima, Mikami, Flockerzi, Takahashi, Kangawa, Kojimi, Matsuo, Hirose & Numa, 1987; Pizarro, Brum, Fill, Fitts, Rodriguez, Uribe & Rios, 1988). It has been proposed that at least some of the DHP receptors constitute the voltage sensors which receive the voltage change of the T-tubular membrane and initiate the transmission of information to the sarcoplasmic reticulum (SR) to cause release of stored Ca^{2+} ions. According to one interpretation of the existing experimental evidence these voltage-sensing molecules are identical with the channel proteins that generate the slow Ca^{2+} inward current (Lamb & Walsh, 1987; Tanabe *et al.* 1987; Tanabe, Beam, Powell & Numa, 1988; Bean, 1989). Calcium entry from the external environment has been ruled out as the trigger for Ca^{2+} release by different previous investigations (Lüttgau & Spiecker, 1979; Lüttgau, Gottschalk & Berwe, 1986; Brum, Rios & Stefani, 1988*a*). If the channel molecule is involved in EC coupling then it is merely its voltage sensitivity that is used. To account for the rapid onset of Ca^{2+} release upon depolarization the Ca^{2+} channel would have to perform a fast voltage-dependent conformational change which triggers transmission to the SR before Ca^{2+} enters the cell through the intrinsic permeation pathway of the channel molecule. Here we show that a fast change of state upon depolarization, which is required by the voltage sensor for Ca^{2+} release, is in fact within the abilities of the slow Ca^{2+} channel. During a certain period of time after a single conditioning activation, the channel shows a significantly accelerated response to a depolarizing step which, under normal conditions, leads only to slow opening. We will describe the onset and decline of the condition that allows fast gating and its dependence on the membrane potential. The extent and time course of intramembrane charge movements, which have previously been associated with the voltage sensor for Ca^{2+} release (Melzer, Schneider, Simon & Szücs, 1986; for review see Huang, 1988), remained virtually unchanged by conditioning depolarization. We will discuss possible mechanisms in which the intramembrane charge movements reflect a fast voltage-dependent conformational change of the Ca^{2+} channel molecule which always occurs upon depolarization but leads to current flow only if an additional (slow) modulation of the channel has taken place. This behaviour would be consistent with the Ca^{2+} channel being a bifunctional molecule in which its fast gate is primarily coupled to Ca^{2+} release from the sarcoplasmic reticulum.

Some of the results have been presented in abstracts (Feldmeyer, Melzer, Pohl & Zöllner, 1989*a*, *b*).

METHODS

Preparation

Single-fibre segments were dissected from m. semitendinosus of frogs (*R. temporaria* and *R. esculenta*) which had been killed by decapitation. Mounting and voltage clamping in a double-Vaseline-gap system followed procedures described previously (Kovacs, Rios & Schneider, 1983; Feldmeyer, Melzer & Pohl, 1990). The fibres were not stretched because the high chelator concentration in the 'internal solution' prevented contraction. The measured sarcomere length was between 1·9 and 2·1 μm.

Solutions

External and internal solutions were similar to those used by Garcia & Stefani (1987) for studying Ca^{2+} currents in cut fibres of *R. pipiens*. The constituents were as follows.

External solution (in mM): $Ca(CH_3SO_3)_2$, 10; $TEA(CH_3SO_3)_2$, 120; TEA–HEPES, 2; 4-aminopyridine, 1; TTX, $3{\cdot}1 \times 10^{-4}$ (pH 7·4).

Internal solution (in mM): caesium glutamate, 80; $MgCl_2$, 6·2; CsHEPES, 10; Cs_2EGTA, 20; Na_2ATP, 5; glucose, 5·6; Antipyrylazo III, 0·4 or 0·8 (pH 7·0).

Signal recording

Electrical recording and data acquisition followed the procedure outlined in a previous paper (Feldmeyer *et al.* 1990). The effective linear capacitance of the fibre was determined at the beginning of the experiment at a holding potential of 0 mV by 100 ms pulses to +60 mV. Most of the linear capacitive and ionic leak currents were removed before analog–digital conversion by analog subtraction of a signal produced by a transient generator (Hille & Campbell, 1976). Current signals were filtered by an 8-pole Bessel filter set at a corner frequency appropriate for the respective digital sampling rate which ranged from 100 to 1000 Hz. Calcium current recording started about 60 min after applying the internal solution to the end-pools and the external solution to the middle pool and 10 min after setting the holding potential to −80 mV. All records shown in this paper are single sweeps corrected using hyperpolarizing control pulses of one-quarter test pulse amplitude ($-P/4$ method). The controls were usually obtained after each test pulse application by averaging four to ten sweeps, which had been applied at intervals of about 5 s. The total time interval between individual test pulse applications was about 3 min. Simultaneously with current recording we measured transmitted light at 700 and 850 nm as described previously (Feldmeyer *et al.* 1990) to check for intracellular changes of free Ca^{2+}, which could be detected by the intracellularly applied metallochromic indicator Antipyrylazo III. In most of the experiments, virtually no Ca^{2+} transients were notable due to the high concentration of intracellular EGTA (end-pool concentration 20 mM).

The experimental temperature ranged between 12 and 16 °C.

RESULTS

Time course of voltage-dependent current activation after a conditioning activation

Figure 1*A* shows the current response to a test pulse of 1·5 s duration applied to +10 mV. The fast activation of a small inward current is followed by the much slower sigmoidal activation of a second, larger inward current which peaks after about 370 ms and then declines slowly. The slow inward current component corresponds to the well-characterized dihydropyridine- and phenylalkylamine-sensitive Ca^{2+} current (Sanchez & Stefani, 1978; Almers, Fink & Palade, 1981). The rapid component resembles the fast Ca^{2+} current described more recently by various laboratories (Cota & Stefani, 1986; Arreola, Calvo, Garcia & Sanchez, 1987; Hencek, Zacharova & Zachar, 1988).

We chose a simple criterion for estimating the initial fast phase in the unconditioned test currents and determined the half-time of the remaining slow phase to describe its kinetics.

We are aware that lumping the kinetic changes into the behaviour of the single parameter half-time does not fully account for the complexity of the activation kinetics, but it is a convenient and model-independent way of describing the basic overall changes. An alternative approach, which we considered, would be fitting the current by an appropriate function to describe changes of free function parameters related to kinetic components of activation. However, we felt that the arbitrariness would be greater when using functions involving a large number of free parameters, which seems necessary to fit the complex time course. In future work we are planning to get back to a functional description of the activation time course to test specific kinetic models on our data.

Since under steady-state conditions the end of the fast current activation was characterized by a drastic fall in the rate of current rise, we chose the point at which the rate of rise had fallen to a certain fraction (generally 50%) of its initial maximal value as a criterion to account for the contribution of the fast current to the total current.

We tested this procedure on synthetic signals consisting of the sum of two exponential functions whose time constants were different by factors of 10 and 20. The amplitude of the fast function was set to values of 10–30% of the total amplitude. Using our simple correction procedure we obtained estimates of the slow half-time which ranged between 1·17 and 0·82 times the real value.

Cota & Stefani (1986) reported that the fast current in adult skeletal muscle showed a negligible inactivation. Therefore we assumed that the fast current is not affected in its amplitude by conditioning depolarizations. Because of its relatively small size an inactivation of the fast phase would cause only minor changes in our results. Likewise, by omitting the correction for the fast phase in some examples we verified that the correction did not affect the results qualitatively.

The remaining part of Fig. 1 shows how the response to the same depolarization step is altered when preceded by various different pulse protocols.

When the current was interrupted almost at its peak (Fig. 1*B*) by a repolarization to −35 mV, a potential close to the threshold of current activation in this fibre, deactivation occurred rapidly; however, upon a second depolarization to +10 mV 300 ms later, the current reached the same value which had been attained at the time of repolarization within a much shorter period of time. This demonstrates that the closure of the channel did not lead back to the initial state immediately, but to a closed state that could be turned faster into an open configuration. In other words: the conditioning activation transformed the channel into a fast gating mode. This state was quite stable. In Fig. 1*C*, the interval separating the pulses was increased to 1·5 s and the current activation at the second pulse still occurred four times faster than during the first pulse. The accelerating effect of a preceding activation disappeared more rapidly when the fibre was repolarized to the holding potential (Fig. 1*D*), but even in this case a second activation after 1·5 s was notably faster than the first one.

Stability of the fast gating condition at different potentials

On comparing Fig. 1*C* and *D*, it becomes obvious that the membrane potential during a fixed time interval between the conditioning pulse and the test pulse influences the effectiveness of the first pulse on the current response at the second

pulse. The experiment shown in Fig. 2*A* investigates this voltage dependence in greater detail.

The conditioning and test pulse were identical in amplitude and duration. The duration was just sufficient to reach the maximum of the current during the

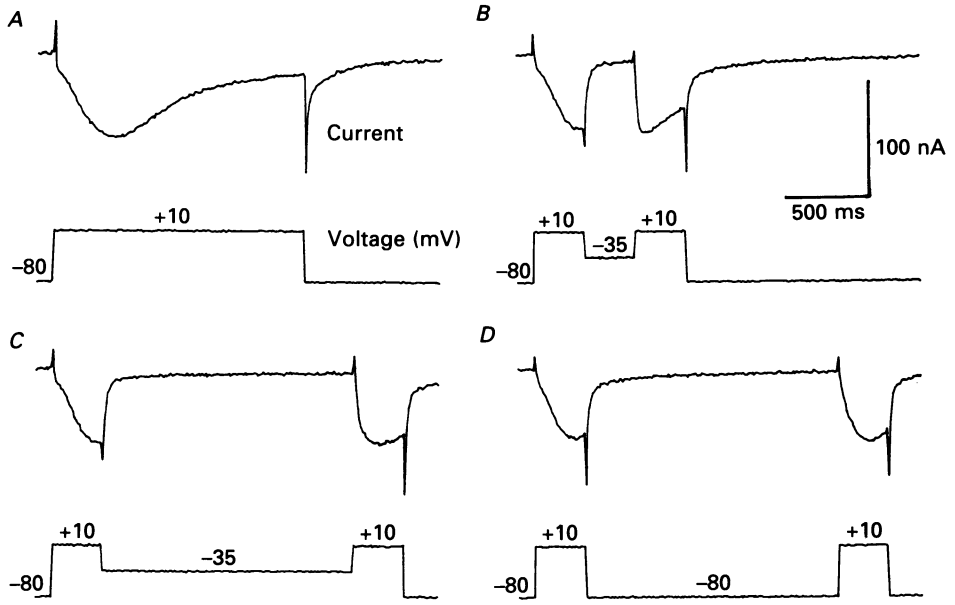

Fig. 1. Modified rate of Ca^{2+} current activation by preceding activation. *A*, inward current caused by a depolarizing voltage step to +10 mV of 1·5 s duration. *B–D*, dual activation by 300 ms pulses to +10 mV, which were separated by an interval of 300 ms at −35 mV (*B*), 1·5 s at −35 mV (*C*) and 1·5 s at −80 mV (*D*). The ratios of the activation half-times (second pulse/first pulse) were 0·16 (*B*), 0·26 (*C*) and 0·58 (*D*). Fibre 170, effective capacitance 14·7 nF, temperature 13 °C.

conditioning pulse. Therefore the conditioning pulse could be used as a control for determining the speed of activation at +20 mV under steady-state conditions. In the experimental series shown in Fig. 2*A*, a fixed interval of 200 ms separated the two pulses, and the potential during the interval varied between −80 and −35 mV, the latter being close to the activation threshold. It is clearly notable that the more positive the interpulse potential the faster the activation of the test current occurred.

In Fig. 2*B* the half-time of activation is plotted against the pre-pulse voltage (V_P). It is obvious that the half-time during the test pulse (●) is always considerably lower than during the conditioning pulse (○).

The control half-times during the conditioning pulse also decreased from 137 to 103 ms. This reflects a change developing slowly with time because going from left to right corresponds to the chronological order in this experimental sequence.

In most cases the activation under steady-state conditions became somewhat faster during the course of an experiment. The reason for this is not entirely clear; the waiting interval between individual pulse applications (3–4 min) might not be quite long enough to completely re-establish

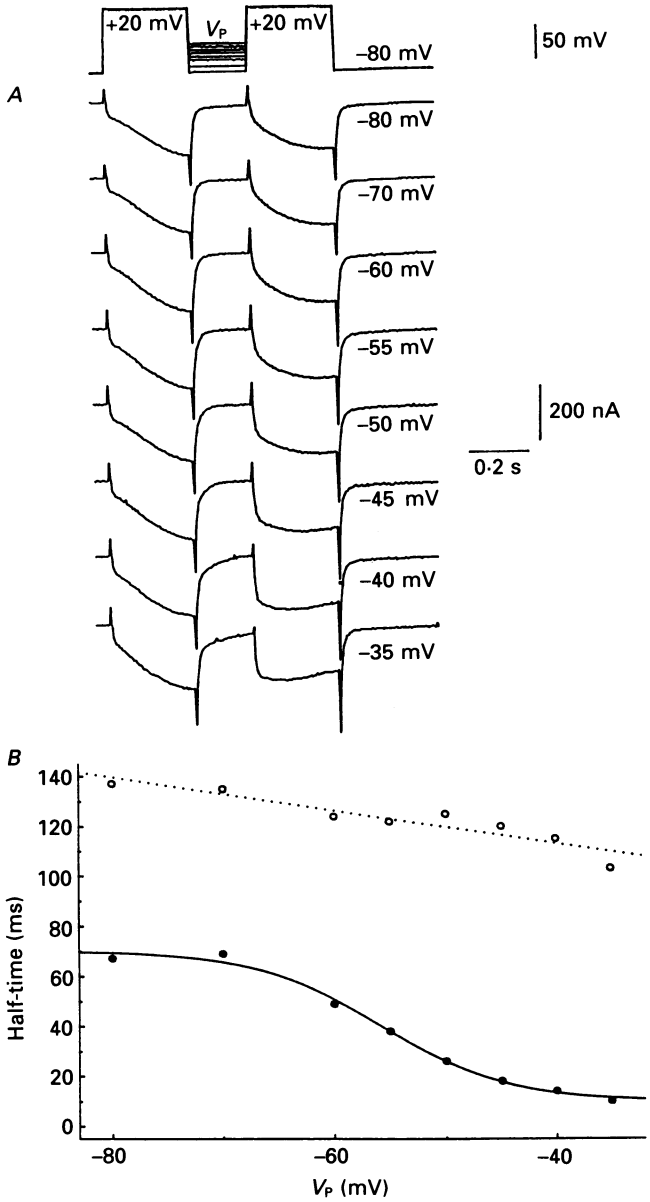

Fig. 2. Dependence of the time course of inward current activation during a test pulse (V_T) on the potential V_P in the interval between a conditioning pulse (V_C) and the test pulse. *A*, current records obtained by the voltage-clamp pulses shown at the top. Conditioning and test pulse had a duration of 300 ms. The voltage during the 200 ms interval between both pulses was varied according to the values on the right. *B*, half-time of current activation during the second pulse (●) for the sequence shown in *A* as a function of the interpulse potential V_P. The open circles represent half-times obtained from the corresponding conditioning pulses. The non-zero slope of their voltage dependence results from a gradual change of the current kinetics with time. During the sequence shown here which covered a time period of 197 min, the half-time decreased from 137 to 103 ms (see also text). Fibre 180, diameter 196 μm, segment length 455 μm, effective capacitance 27·1 nF, temperature 12·6 °C.

the initial conditions but the slow change may also result from the wash-out of a regulatory component.

In Fig. 3 the half-times of the test currents were referred to each corresponding control half-time obtained from the conditioning pulse. The fractional recovery at five different pre-pulse intervals (50–1000 ms) is plotted against the pre-pulse

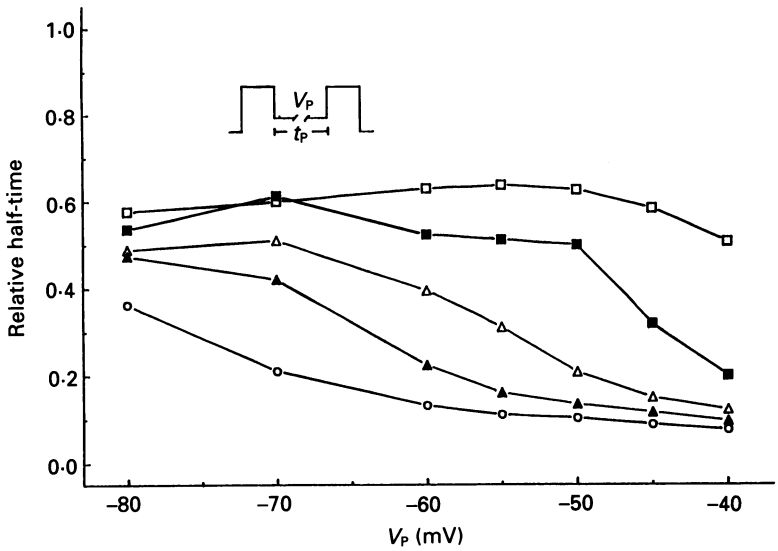

Fig. 3. Fractional restoration of the slow half-time of activation as a function of the potential during the interval between the conditioning and test pulse. Each symbol corresponds to a different interval duration (t_P): □, 1000 ms; ■, 500 ms; △, 200 ms; ▲, 100 ms; ○, 50 ms. Same fibre as in Fig. 2.

potential. For the shorter intervals a more negative potential led to a greater extent of recovery. However, at the longer intervals it becomes evident that the degree of fractional recovery seems to reach an upper limit (about 60%) which cannot be overcome by increasing the potential.

Time course of restoration from the effect of a conditioning activation

In Fig. 4, the relative half-time of activation during the test pulse is plotted against the time interval between conditioning pulse and test pulse. Shortly after time zero, which represents the end of the conditioning pulse, the half-time is down to a small fraction of the steady state (1·0 on the ordinate), and the curves show the recovery at different potentials from this low value towards the large steady-state value. There is a gradual transition from a very slow recovery of the half-time at −35 mV to a rapid initial recovery at −70 and −80 mV. About 50% of the large steady-state half-time is regained within 100–200 ms at the most negative potentials, but then recovery proceeds with a much slower time course which requires intervals of more than a minute between individual pulse applications for complete recovery.

Apparently, more than one process is involved in the restoration of the steady-state conditions following a strong activation: one process that is clearly voltage-dependent and much faster at more negative potentials, and a second considerably

slower process which could not be resolved in the time frame used in these experiments.

Conditioning by subthreshold pre-pulses

In the type of experiment shown in Fig. 5, we investigated the question of whether a subthreshold pre-depolarization could cause a condition similar to the one

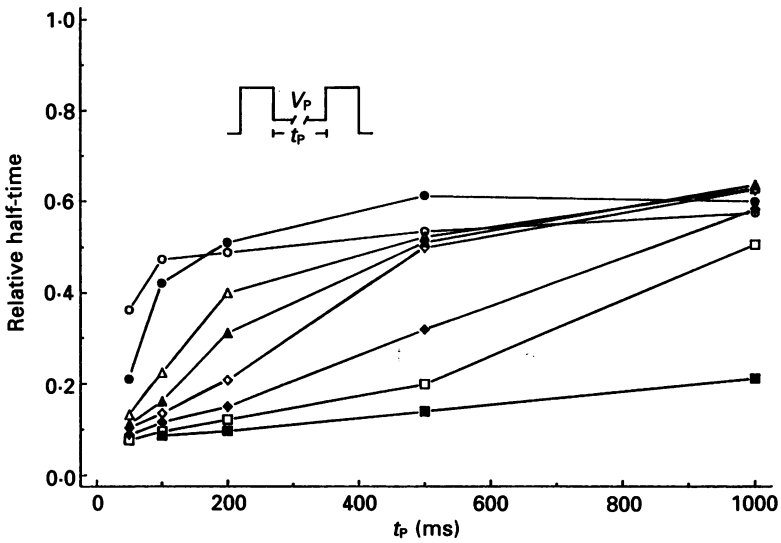

Fig. 4. Restoration of the slow activation time course for a test pulse applied at different times after a previous activation. Each symbol corresponds to a different voltage (V_P) in the interval between conditioning and test pulse: ○, −80 mV; ●, −70 mV; △, −60 mV; ▲, −55 mV; ◇, −50 mV; ◆, −45 mV; □, −40 mV; ■, −35 mV. Same fibre as in Figs 2 and 3.

produced by a large preceding activation, i.e. in which the turn-on kinetics of the Ca^{2+} current were faster. We used two pre-pulse potentials (−50 and −40 mV), and the pulse protocol shown in Fig. 5*A*. In all cases, the test pulse was a depolarization to 0 mV lasting for 1 s. It was preceded either by a simple step to the pre-pulse potential or by a large activating pulse to +40 mV lasting for 120 ms followed by a repolarization to the pre-pulse potential, which was then maintained for different periods of time.

The lower traces in Fig. 5*B* (◇ and ◆) show the partial recovery of the half-time with increasing distance from the conditioning pulse, which has already been demonstrated in Fig. 4. The upper trace (○) shows the effect of a subthreshold pre-depolarization at −50 mV. This pre-pulse potential had obviously no effect on the time course of the test activation. Even holding the membrane for 12 min at −50 mV did not change the test pulse response in any significant way (not shown). A pre-pulse potential 10 mV more positive, however, caused an acceleration in the turn-on of the test current (●). After 3 s, the two curves (with and without conditioning activation) measured at the pre-pulse potential of −40 mV (dashed lines) approached a similar value for the half-time.

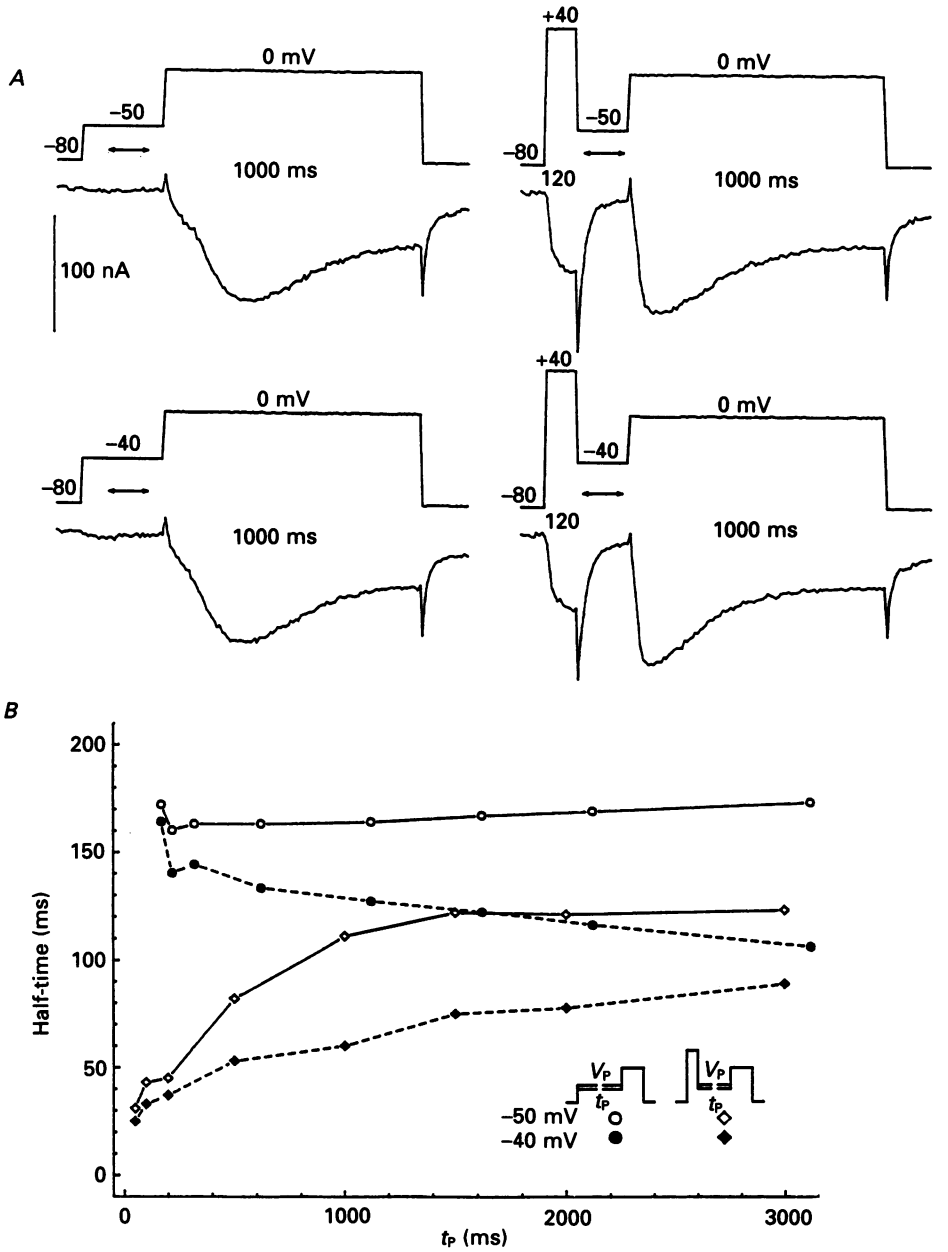

Fig. 5. Influence of subthreshold pre-pulses on the activation kinetics. *A*, pulse protocol for studying the effect of subthreshold pre-pulses (to −50 and −40 mV) of different duration on the activation speed of the test current (records on the left). In the same fibre the pulse protocol of Fig. 4 was carried out to study the time course of recovery from the fast gating mode at the two subthreshold pre-pulse potentials (records on the right). *B*, half-time of current activation during the test pulse as a function of the pre-pulse duration (○ and ●) or inter-pulse duration (◇ and ◆). Fibre 194, diameter 144 μm, segment length 595 μm, effective capacitance 21·9 nF, temperature 15 °C.

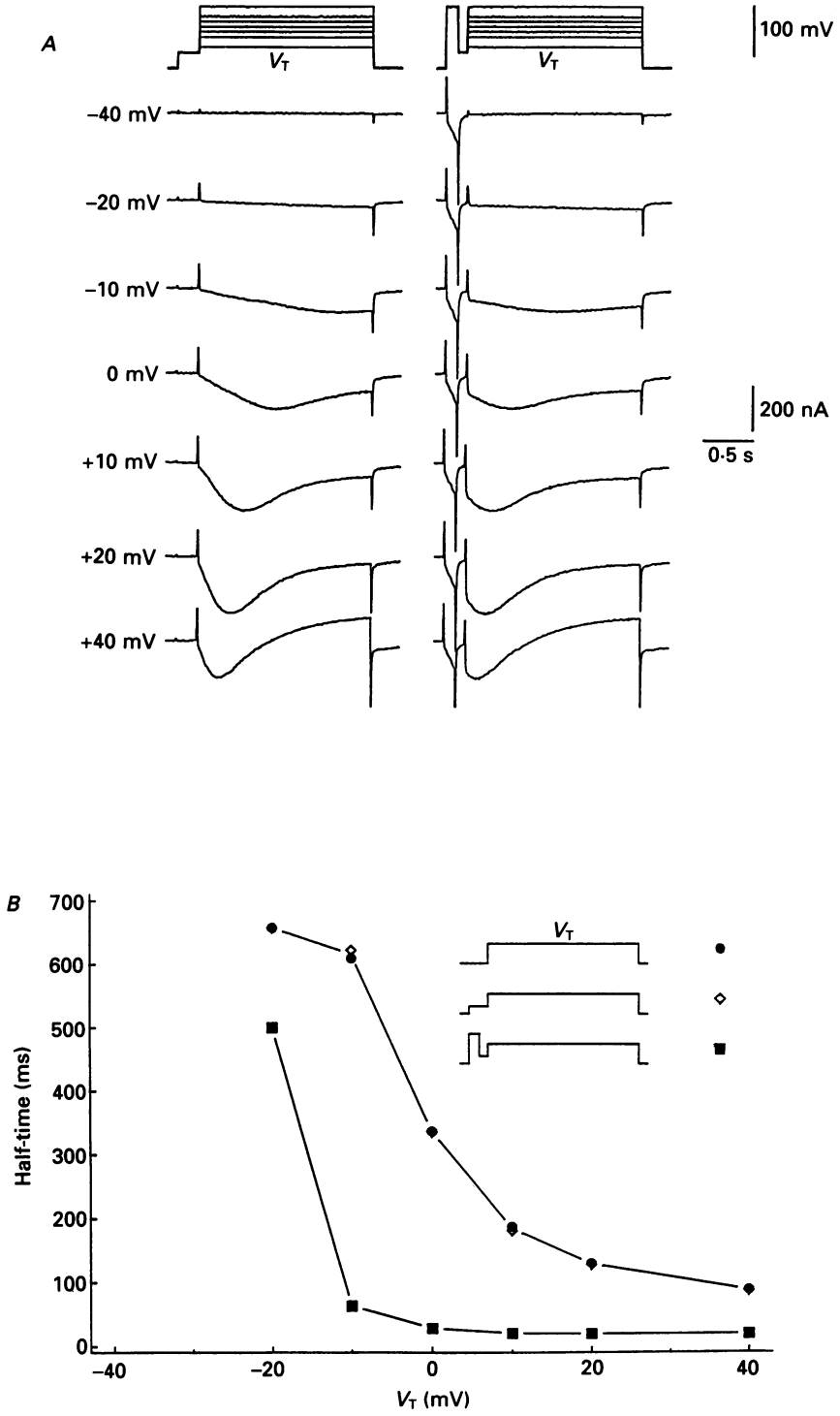

Fig. 6. For legend see facing page.

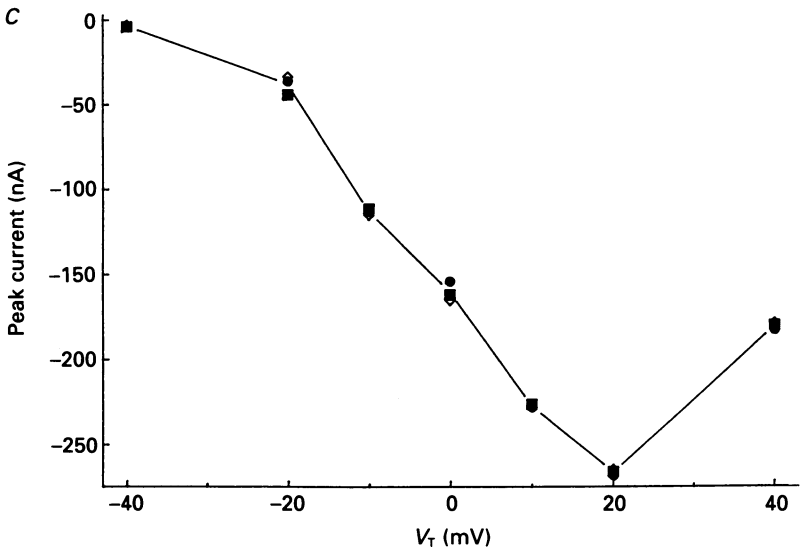

Fig. 6. Voltage dependence of Ca^{2+} currents which were modified by a previous activation. *A*, test pulses of 1·78 s duration were applied to potentials (V_T) ranging from −40 to +40 mV. Each pulse was applied after a 220 ms subthreshold pre-depolarization to −50 mV (left column), or after a 120 ms pulse to +40 mV which was followed by a 100 ms interval at −50 mV (right column). *B*, half-time to the current maximum of the records shown in *A* as an inverse measure of the speed of activation plotted against the test pulse amplitude, V_T. Note the much smaller activation half-times after the conditioning activation. The inset relates the pulse programme used to the graphical symbols in *B* and *C*. The diagrams also include data from an additional recording sequence (●) using test pulses without any pre-pulse. *C*, relationship between peak current and the membrane potential, V_T, during the test pulse. Note that most of the values virtually coincide. Fibre 190, diameter 180 μm, segment length 818 μm, effective capacitance 25·3 nF, temperature 15 °C.

Voltage dependence of the currents in the fast gating condition

In Fig. 6 the current–voltage characteristics in the slow and in the fast gating mode are compared. In Fig. 6*A* (right column), a strong conditioning depolarization to +40 mV was applied and interrupted after 120 ms before the current reached its maximum; deactivation was allowed for 100 ms at −50 mV before the test pulse was applied. The test pulse amplitude was changed over a wide range of potentials. The current onset as a response to the test pulse was considerably faster in these records compared with those where a depolarization to only −50 mV was applied 220 ms prior to the test pulse (Fig. 6*A*, left column). Figure 6*B* quantifies the activation kinetics in terms of the half-time to the peak. Again, it can be seen that the subthreshold depolarization on its own caused no change when compared with records (not shown) where the test potentials were applied directly from the holding potential (see also Fig. 5), while the conditioning activation led to a sharp drop in the activation half-time. However, the current–voltage relation for the peak current

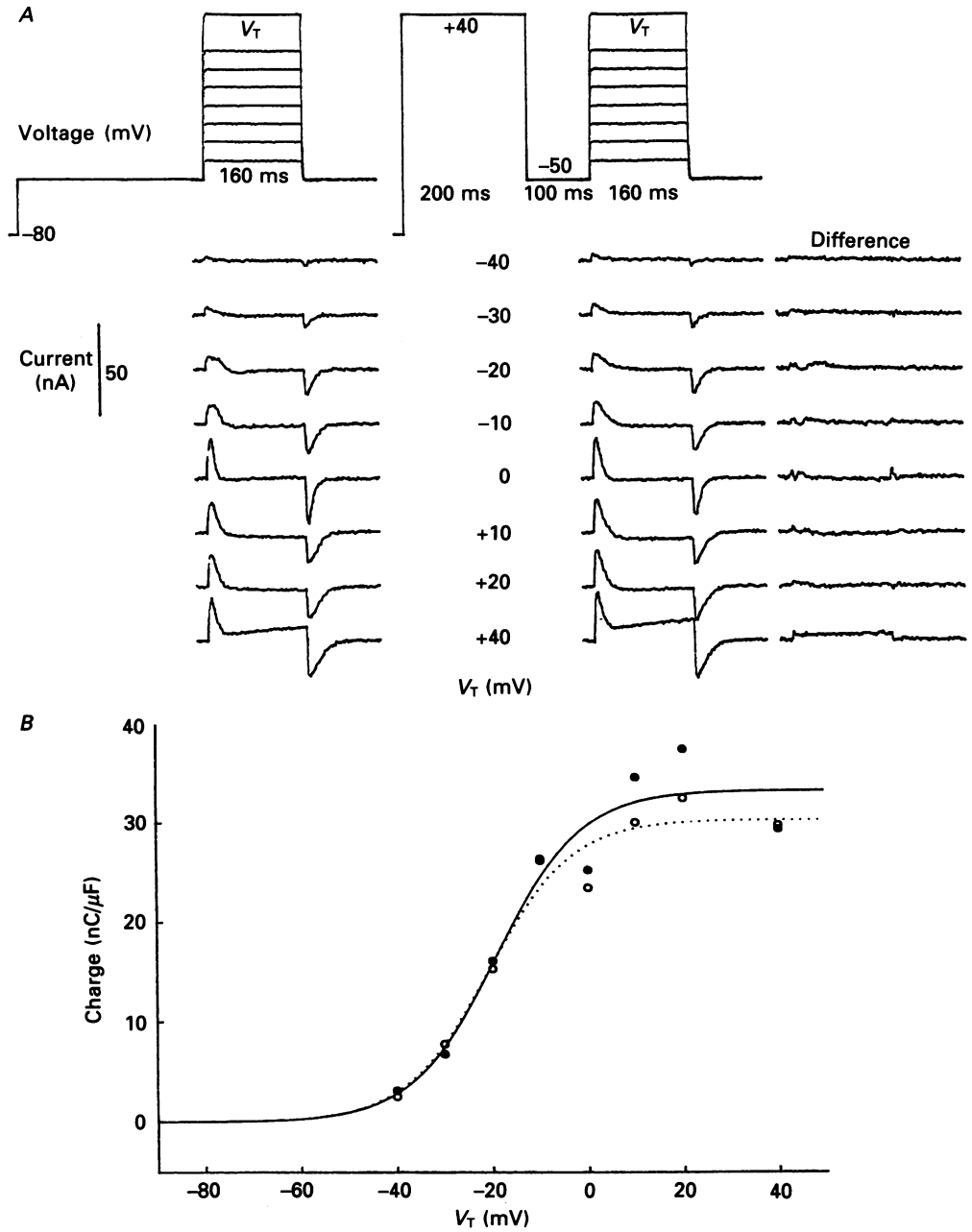

Fig. 7. Effect of conditioning depolarization on intramembrane charge movements at different test pulse voltages, V_T. The external solution contained no Ca^{2+} and 2 mM-Cd^{2+}. *A*, charge movements during test pulses which followed 300 ms after a step to −50 mV (left column) were compared with the response to pulses of identical size and duration (middle column) which were applied 100 ms after the end of a conditioning depolarization to +40 mV, lasting for 200 ms. The potential in the interval between the conditioning and

(Fig. 6*C*) was completely unaffected by the conditioning pulse protocol. This result makes it unlikely that a new channel population exhibiting fast kinetics becomes activated in addition to the slow channels under these circumstances. If this were the case the total current should be larger. Rather, it seems that the same channels which normally open slowly exhibit fast kinetics under the influence of a previous activation.

Intramembrane charge movements studied with conditioning pulses

According to one hypothesis, the voltage sensor for EC coupling and the slow Ca^{2+} channel may be one and the same molecule (Bean, 1986; Tanabe *et al.* 1987). If this is correct, the intramembrane charge movements, which have previously been mainly correlated with EC coupling, are likely to be involved in both the gating of Ca^{2+} release from the SR and the gating of the slow Ca^{2+} channel. Even if the Ca^{2+} channels constitute a different group of molecules not involved in EC coupling they should, as voltage-dependent pores, exhibit gating charge movements. In either case the drastic change in the gating kinetics of this channel, which is caused by a conditioning activation may also be reflected in a change of charge movements kinetics. We investigated this question by comparing charge movements with and without a conditioning pulse. We measured charge movements using a conditioning pulse protocol that caused a considerable change in the activation kinetics of the Ca^{2+} current. After verifying this in a Ca^{2+}-containing solution, we replaced Ca^{2+} by Cd^{2+} (2 mM) to eliminate the ionic inward current. The non-linear currents were determined by the same procedure ($-P/4$ method) that was used for determining Ca^{2+} currents. The pulse protocol used in the experiment of Fig. 7 was virtually the same as that in Fig. 6, only the test pulses were shorter. In Fig. 7*A*, steps of 160 ms duration were applied to a variety of potentials between -40 and $+40$ mV, each starting at a pre-pulse level of -50 mV. In the sequence on the right, a conditioning depolarization to $+40$ mV lasting 200 ms was applied starting 300 ms before each test pulse. Only test pulse responses were sampled and are shown in the figure. The right-most column shows the results of subtracting each test current obtained without conditioning pulse from the corresponding test current with conditioning pulse. To determine the charge moved by the test pulse we fitted straight sloping lines to the last 100 ms of the current during the pulse and during a 60 ms interval starting 60 ms after pulse-off. The lines were extrapolated to the preceding pulse edge and subtracted from the records. On- and off-charges (i.e. the integral of the current of the first 60 ms during the pulse and the first 60 ms after the pulse) were averaged and normalized by the linear capacitance. The values are plotted against the test

---

the test pulse was set to -50 mV. The right column shows the difference obtained by subtracting the current without the conditioning pulse from the current with the conditioning pulse. *B*, charge–voltage relations using the data of *A*. The curves represent non-linear least-squares fits of the Boltzmann distribution $Q = Q_{max}/(1-\exp((\bar{V}-V)/k))$ to each group of data points. ●, ——, records with conditioning pulse (Q_{max} = 33·2 nC/μF, k = 8·8 mV, $\bar{V} = -19{\cdot}2$ mV); ○, ····, records without conditioning pulse (Q_{max} = 30·3 nC/μF, k = 8·7 mV, $\bar{V} = -20{\cdot}8$ mV). Fibre 192, diameter 137 μm, segment length 471 μm, effective capacitance 12·5 nF, temperature 15–16 °C.

pulse potential in Fig. 7*B* and were fitted using a conventional two-state Boltzmann distribution (see the figure legend).

The procedure used here is comparable to that used in previous measurements of charge movements above the voltage threshold for Ca^{2+} release (Melzer *et al.* 1986). A potential problem using this procedure is the presence of some non-linear charge in the negative voltage region (here −87·5 to −110 mV) where the control pulses were obtained (Brum & Rios, 1987; Feldmeyer *et al.* 1990) which may cause a certain distortion of charge movement records, depending on the slope of the absolute charge–voltage relation (Adrian & Almers, 1976) and the time course of the charge movements contaminating the controls.

To exclude any influence of the controls when studying the effect of the conditioning pulse we also subtracted the total test current without the conditioning pulse directly from the corresponding records with the conditioning pulse. The records obtained in this way were indistinguishable from the difference records in Fig. 7*A*. The difference records exhibit small bumps at potentials between −20 and 0 mV but it is questionable whether this reflects a change in intramembrane charge movements. Small residual ionic currents could easily cause noise signals of this size. Likewise the difference in the charge–voltage relation between 0 and +20 mV was caused by slowly sloping currents of very small amplitude and probably does not indicate a real change in the displacement current.

It can therefore be noted that no significant change in the charge movements occurs under the influence of a conditioning depolarization which drastically alters the current kinetics. However, small alterations at the edge of our detectability cannot be ruled out.

DISCUSSION

Response of Ca^{2+} current and intramembrane charge movement to conditioning depolarization

The feature by which the main Ca^{2+} current of skeletal muscle differs strikingly from other channels of the same pharmacological sensitivity is its remarkably slow opening response upon depolarization. The present study showed that the channel has the intrinsic ability to quickly respond to membrane potential changes. This fast gating mode, however, becomes apparent only during a limited time after a conditioning activation. A voltage-dependent process seems to determine the transition to the fast gating mode exhibiting a voltage threshold which is rather close to the activation threshold of the current (Fig. 5). At the threshold, even though negligible current was activated, a gradual increase in the gating speed could be observed (Fig. 5). Much more effective, however, was a strong conditioning depolarization which caused an almost maximal activation of the current.

The data of Fig. 4 indicate a complex time course, involving at least two processes, of the return to the normal gating mode from the fast gating condition attained by a conditioning activation. One of these processes is clearly dependent on membrane potential and exhibits a half-time of less than 100 ms at the holding potential of −80 mV, but it becomes progressively slower at more positive potentials. It is interesting to note that subthreshold potentials (e.g. −50 mV), which were not

sufficient to transform the system into the fast gating mode by themselves, were nevertheless effective in decelerating the restoration of the slow gating mode (Fig. 5). The second process, which finally resets the initial conditions, is so slow that, in a time frame of a few seconds after the conditioning pulse, a quasi steady state of accelerated gating kinetics prevails (Fig. 4).

It seems natural to link the slow recovery processes discovered in our dual activation experiments to the slow opening kinetics exhibited by the channels in the steady state. Our experiments allow no conclusion regarding the underlying mechanisms of the slow reactions, which are involved in the function of the Ca^{2+} channels, but we think it is worthwhile when conducting further experiments to consider possible modulatory effects of the environment. In this context it is interesting to note that cyclic AMP and adrenaline caused a decrease in the time to peak of the slow Ca^{2+} current (Arreola *et al.* 1987).

Considering the kinetics of the fast steady-state current component which we assumed to be unchanged by a conditioning depolarization (Cota & Stefani, 1986), one may wonder if the effect of a conditioning pulse is not an enhancement of this current. This cannot be ruled out so far but we never observed an increase of the total current amplitude which could explain the fast current rise as an additional recruitment of new channels. So if an enhancement of the fast current takes place it has to go along with a simultaneous suppression of the slow current. This brings about the interesting possibility that the fast phase seen in the normal unconditioned current is not generated by a separate channel population but by a fraction of the slow channels showing fast gating kinetics already in the steady state. Further experiments are required to clarify this point.

We found no significant change in the non-linear capacitive current when a large conditioning depolarization was applied. On the other hand Brum, Fitts, Pizarro & Rios (1988*b*) reported a potentiation in charge movement up to about 170% when applying pulse protocols similar to ours for studying the time course of charge inactivation. Since the external solution used in that study contained millimolar concentrations of free Ca^{2+} and no attempt had been made to block the Ca^{2+} current, an apparent increase in charge movement may well have occurred under those conditions merely due to the altered kinetics of the Ca^{2+} current, which were demonstrated in the present investigation.

Implication of the current kinetics for normal muscle function

The normal electrical signal in working muscle is a large brief depolarization by an action potential or a train of such action potentials causing repetitive or tetanic contractions. The properties of the Ca^{2+} channel described in this paper constitute a 'track-and-hold' system that allows effective summation of channel opening from one spike to the next. During repetitive excitation, accumulative opening will occur much faster than one would expect if the channel returned to its ground state with the time course of closure. Due to the strong voltage dependence of the time course of restoration (see Fig. 4), a maintained slight depolarization in the spike intervals, for instance caused by the negative after-potential (Adrian, Chandler & Hodgkin, 1970), would enhance summation.

During repetitive stimulation Ca^{2+} release from the sarcoplasmic reticulum is

partially inactivated (Baylor, Chandler & Marshall, 1983). This inactivation seems to be caused by a negative feedback of released Ca^{2+} on the release mechanism (Schneider & Simon, 1988) whose physiological role may be prevention of excessive loss of Ca^{2+} from the storage sites. A delayed increase of Ca^{2+} influx via the DHP-sensitive Ca^{2+} channel during repetitive excitation may be of functional significance in supporting the Ca^{2+}-dependent inactivation of the release channels and in compensating for any loss of Ca^{2+} to the outside occurring during the Ca^{2+} transient.

Models for the kinetic behaviour of the channels

A quantitative description of activation and inactivation of the slow Ca^{2+} current has been given by Sanchez & Stefani (1983) in terms of a Hodgkin–Huxley-type of formalism (Hodgkin & Huxley, 1952). We used their published parameters in an attempt to simulate the system behaviour reported in the present paper. Even though activation and inactivation kinetics as responses to a single voltage step could be simulated satisfactorily, the model failed to reproduce the long-lasting memory of the channel for a previous activation. If inactivation is disregarded (which can be done for simplicity since its rate is relatively small), activation in the Sanchez–Stefani model corresponds to a sequential four-state scheme (Fig. 8*A*) in which the rate constants k_{ij} (mediating the transition from state i to state j) are multiples of only two voltage-dependent rate constants, α and β: $k_{12} = 3\alpha$, $k_{23} = 2\alpha$, $k_{34} = \alpha$, $k_{21} = \beta$, $k_{32} = 2\beta$, $k_{43} = 3\beta$ (see Hille, 1984). With regard to a general sequential activation scheme White & Bezanilla (1985) pointed out that, in double-pulse experiments similar to the ones used here, the time required for activation at the second pulse will be shorter if the last step (i.e. the closed–open transition) is not rate limiting. For instance, if all closed–closed transitions were slow but the last transition to the open state was fast (Fig. 8*A*), one would get a slow opening on depolarization and a fast closing on repolarization but a slow return to state 1. Some time after repolarization, a certain number of channels would still occupy state 3 and could be opened rapidly on a second depolarization. Apparently in the Sanchez–Stefani model, the rate constants of the last transition are not sufficiently large relative to the other rate constants to simulate the observed behaviour of the current.

Possible explanations for the behaviour of both the current and the charge movements

The intramembrane charge movements showed virtually no sensitivity to a conditioning pulse which altered the activation dynamics of the Ca^{2+} current.

As a voltage-dependent process the current has to be associated with a gating charge movement. The strong voltage dependence of the opening kinetics (Fig. 6*A*, left column, and Fig. 6*B*) indicates a dipole moment change during the transition to the open state. Since this transition occurs much more quickly after a conditioning pulse one might expect a considerable relative increase in the gating current amplitude. A possible explanation for the lack of change in the intramembrane charge recordings could be that the gating charges associated with opening of the Ca^{2+} channel were very small so that they are not resolvable. It has been shown in previous work that obviously only a small fraction of the DHP receptors in skeletal muscle conducts Ca^{2+} during a depolarization (Schwartz, McCleskey & Almers, 1985).

This could indicate that only a few of the DHP receptors are in fact Ca^{2+} channels which exhibit a high open-state probability at large depolarization while the vast majority are structurally different and never open (Schwartz *et al.* 1985). Another possibility would be that all DHP receptors are structurally identical Ca^{2+} channel

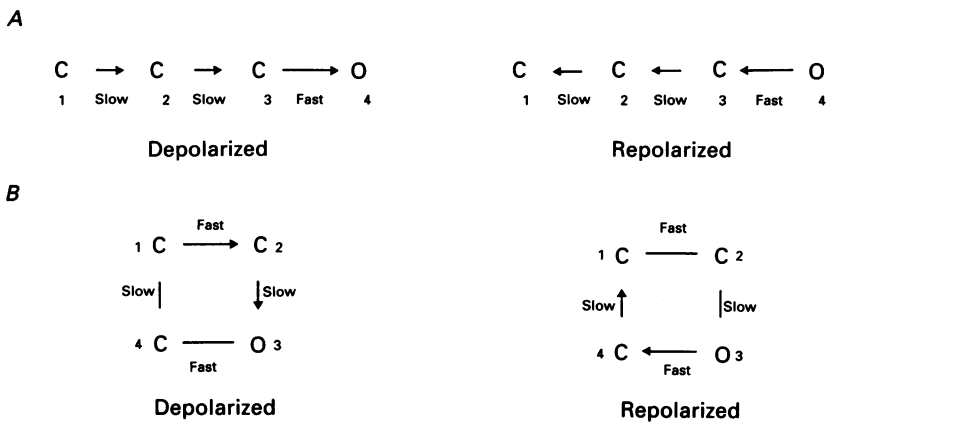

Fig. 8. State diagrams which qualitatively produce the kinetic behaviour of the current described in this paper (slow and fast gating mode). The arrows indicate the predominating transitions occurring after changing the membrane potential from a sufficiently negative value to a considerably more positive value ('depolarized') and vice versa ('repolarized'). Scheme *B* would always produce the same (measurable) fast gating current regardless of the current kinetics if there were the same voltage-dependent rate constants between states 1 and 2 and between states 4 and 3. A similar charge movement behaviour could be found in a sequential scheme like *A* if the transition $1 \rightarrow 2$ was not slow, as drawn here, but fast and voltage dependent, and states 3 and 4 occurred with small probability so that any fast charge movements in the $3 \rightarrow 4$ transition would contribute little to the total charge. See text for further information.

molecules which, however, exhibit a very small open-state probability even at large depolarization (Lamb & Walsh, 1987). A large fraction of intramembrane charge is sensitive to phenylalkylamines and dihydropyridines (Hui, Milton & Eisenberg, 1984; Lamb, 1986; Rios & Brum, 1987; Pizarro *et al.* 1988; Feldmeyer *et al.* 1990). On the other hand, most of the intramembrane charge measurable above -50 mV has been correlated with the rate of Ca^{2+} release (Melzer *et al.* 1986) and the sensitivity of charge movements to Ca^{2+} antagonists is similar to that of Ca^{2+} release (Rios & Brum, 1987; Feldmeyer *et al.* 1990). Therefore, probably a large fraction of the charge movements shown in Fig. 7 belongs to DHP receptors, i.e. proteins that contain the α_1 subunit carrying high-affinity DHP binding sites (Tanabe *et al.* 1987; Campbell, Leung & Sharp, 1988), and those DHP receptors function as voltage sensors for SR Ca^{2+} release. They may have only this function or they could in addition form Ca^{2+} pores.

We can think of three possibilities to accommodate those results with our finding that the charge movements show no change when the current activates faster.

(1) If two classes of DHP receptors exist, the measurable charge movements belong to those which are not Ca^{2+} channels. They may behave in a kinetically different way from the Ca^{2+} channels whose gating currents may not be resolvable.

(2) If a homogeneous population of DHP receptors exists, the measurable charge movements may originate from a fast transition between closed states which is carried out by a much larger number of molecules than those which open. A sequential scheme like the one in Fig. 8*A* can explain this behaviour if the energies of states 3 and 4 remain high relative to 1 and 2 even at large depolarizations; then only a small fraction of the channel population gets into the fast gating mode; the bulk of the channels perform just the closed–closed transition between states 1 and 2. If this transition is fast (rather than slow as drawn in the scheme) the charge movement component associated with this transition will be dominating and conditions which lead to large relative changes in the current need not necessarily change these charge movements.

(3) The kinetic mechanism of the Ca^{2+} channels is such that the same fast charge movement takes place whether they operate in the slow or in the fast gating mode.

A reaction scheme that shows this property and which reproduces the basic results of our conditioning pulse experiments is shown in Fig. 8*B*. It assumes that the Ca^{2+} pore is controlled by a fast voltage-dependent process and by a second slow reaction whereby opening requires the action of both mechanisms in conjunction. The horizontal transitions ($1 \rightarrow 2$ and $4 \rightarrow 3$) represent the fast gate and the vertical transitions ($1 \rightarrow 4$ and $2 \rightarrow 3$) the slow gate. At the resting potential, the system is in state 1. A depolarization causes a fast transition to state 2 and subsequently a slow movement to state 3 accompanied by opening. On repolarization, the system moves along a different pathway: first to state 4 leading to fast closing and slowly back to state 1. After repolarization, state 4 is relatively stable, allowing fast opening (via the $4 \rightarrow 3$ transition) on a second depolarization. If the activation energy differences at zero voltage and the dipole moment change between states 1 and 2 and between states 4 and 3 are the same, the charge movement generated by the $1 \rightarrow 2$ transition and by the $4 \rightarrow 3$ transition will be indistinguishable. Charge movements may also occur in the vertical transitions but will be relatively slow and therefore generate small slowly declining currents, which would probably be considered as small ionic current contaminations under most experimental conditions. Therefore this model generates always virtually the same measurable gating current regardless of which fraction of the total channel number is in the fast gating mode. In its simplest form, the model has the same set of voltage-dependent rate constants in both horizontal transitions ($k_{12} = k_{43}$ and $k_{21} = k_{34}$) and in both vertical transitions ($k_{23} = k_{14}$ and $k_{32} = k_{41}$); it then corresponds to a pore whose opening state is controlled by two charged particles, each performing independent and kinetically different transitions between a resting and a gated state with the pore only being open when both particles are in the gated state.

The Ca^{2+} channel as a possible voltage sensor for EC coupling

Our experimental observations may not only be of significance to complement the existing functional information about the slow Ca^{2+} channel in skeletal muscle; they may also provide an important piece of information regarding EC coupling.

Calcium channel antagonists have repeatedly been reported to affect EC coupling (Eisenberg, McCarthy & Milton, 1983; Hui *et al.* 1984; Berwe, Gottschalk & Lüttgau,

1987; Rios & Brum, 1987; Erdmann & Lüttgau, 1989; Feldmeyer *et al.* 1990) indicating a role of DHP receptors in the control of Ca^{2+} release. It is possible that the α_1 polypeptide, which has the primary structure typical for channel proteins (Tanabe *et al.* 1987), is part of a bifunctional protein that forms a voltage sensor for calcium release from the sarcoplasmic reticulum and exhibits a calcium permeability (Bean, 1989). A result pointing to this possibility, even though not unequivocally, is the simultaneous restoration of EC coupling and slow Ca^{2+} current in dysgenic mouse muscle after injection of cDNA encoding the rabbit α_1 subunit (Tanabe *et al.* 1988). A scheme like the one in Fig. 8*B* can provide a model for a bifunctional molecule that controls two kinetically different processes. Rapid voltage control of Ca^{2+} release could be performed via the fast gate associated with rapid charge movement. Our results show that the Ca^{2+} channel molecules can in principle react quickly upon depolarization, which is a necessary requirement for any possible control element of intracellular Ca^{2+} release.

The rate of Ca^{2+} release caused by a depolarization to +20 mV at 7·5 °C requires slightly more than 10 ms to reach its maximum (Simon & Schneider, 1988). The smallest half-times for the activation of the inward current in our experiments were about 10 ms (at 12–16 °C); however, using the single parameter half-time for quantifying the kinetics underestimates the speed of the most rapid component in the accelerated current, because in most cases the activation time course still contained a slow component in addition to the rapid phase (see, for instance, Fig. 6*A*). Therefore the rapid opening after conditioning activation may well reveal a conformational change of the Ca^{2+} channel molecule which is normally coupled to the control of Ca^{2+} release but silent in terms of Ca^{2+} conductance.

In the fast gating mode of the skeletal muscle Ca^{2+} current the speed of activation is comparable to that of Ca^{2+} channels in other tissues, for instance heart muscle (McDonald, Cavalie, Trautwein & Pelzer, 1986), showing similar pharmacological properties (L-type). The primary structure of the cardiac channel has been shown to exhibit the same general pattern as the skeletal muscle α_1 subunit but many differences in detail (Mikami, Imoto, Tanabe, Niidome, Mori, Takeshima, Narumiya & Numa, 1989). Therefore, even though the channel proteins of heart and skeletal muscle are similar in terms of their drug sensitivity and Ca^{2+} permeability the genes that encode both systems are different. The modulation that causes the fast gating mode in our experiments may functionally reverse a structural modification which determines the kinetic difference between skeletal muscle Ca^{2+} channel and 'conventional' L-type channels. This modification could have evolved in skeletal muscle together with a new control mechanism for intracellular Ca^{2+} release by the T-system membrane potential and may reflect the structural transformation of the Ca^{2+} channel into a voltage sensor for this control device.

We would like to thank Dr H. Ch. Lüttgau for critical reading of the manuscript and stimulating discussions, Dr G. Boheim and Dr G. D. Lamb for encouragement and helpful suggestions, Mr R. Schwalm for skilful programming and assistance with numerical simulations, and Ms E. Linnepe for editorial help. This work was supported by a research grant from the Deutsche Forschungsgemeinschaft (FG Konzell).

REFERENCES

ADRIAN, R. H. & ALMERS, W. (1976). Charge movement in the membrane of striated muscle. *Journal of Physiology* **254**, 339–360.

ADRIAN, R. H., CHANDLER, W. K. & HODGKIN, A. L. (1970). Voltage clamp experiments in striated muscle fibres. *Journal of Physiology* **208**, 607–644.

ALMERS, W., FINK, R. & PALADE, P. T. (1981). Calcium depletion in frog muscle tubules: the decline of calcium current under maintained depolarization. *Journal of Physiology* **312**, 177–207.

ARREOLA, J., CALVO, J., GARCIA, M. C. & SANCHEZ, J. A. (1987). Modulation of calcium channels of twitch skeletal muscle fibres of the frog by adrenaline and cyclic adenosine monophosphate. *Journal of Physiology* **393**, 307–330.

BAYLOR, S. M., CHANDLER, W. K. & MARSHALL, M. W. (1983). Sarcoplasmic reticulum calcium release in frog skeletal muscle fibres estimated from Arsenazo III calcium transients. *Journal of Physiology* **344**, 625–666.

BEAN, B. P. (1986). Calcium channels in skeletal muscle: what do they do? *Trends in Neurosciences* **9**, 535–536.

BEAN, B. P. (1989). More than a Ca^{2+} channel? *Trends in Neurosciences* **12**, 128–130.

BERWE, D., GOTTSCHALK, G. & LÜTTGAU, H. CH. (1987). Effects of the calcium antagonist gallopamil (D600) upon excitation–contraction coupling in toe muscle fibres of the frog. *Journal of Physiology* **385**, 693–707.

BRUM, G., FITTS, R., PIZARRO, G. & RIOS, E. (1988*b*). Voltage sensors of the frog skeletal muscle membrane require calcium to function in excitation–contraction coupling. *Journal of Physiology* **398**, 475–505.

BRUM, G. & RIOS, E. (1987). Intramembrane charge movement in frog skeletal muscle fibres. Properties of charge 2. *Journal of Physiology* **387**, 489–517.

BRUM, G., RIOS, E. & STEFANI, E. (1988*a*). Effects of extracellular calcium on calcium movements of excitation–contraction coupling in frog skeletal muscle fibres. *Journal of Physiology* **398**, 441–473.

CAMPBELL, K. P., LEUNG, A. T. & SHARP, A. H. (1988). The biochemistry and molecular biology of the dihdropyridine-sensitive calcium channel. *Trends in Neurosciences* **11**, 425–430.

COTA, G. & STEFANI, E. (1986). A fast-activated inward calcium current in twitch muscle fibres of the frog (*Rana montezume*). *Journal of Physiology* **370**, 151–163.

EISENBERG, R. S., MCCARTHY, R. T. & MILTON, R. L. (1983). Paralysis of frog skeletal muscle fibres by the calcium antagonist D-600. *Journal of Physiology* **341**, 495–505.

ERDMANN, R. & LÜTTGAU, H. CH. (1989). The effect of the phenylalkylamine D888 (devapamil) on force and Ca^{2+} current in isolated frog skeletal muscle fibres. *Journal of Physiology* **413**, 521–541.

FELDMEYER, D., MELZER, W. & POHL, B. (1990). Effects of gallopamil on calcium release and intramembrane charge movements in frog skeletal muscle fibres. *Journal of Physiology* **421**, 343–362.

FELDMEYER, D., MELZER, W., POHL, B. & ZÖLLNER, P. (1989*a*). Altered gating kinetics of the skeletal muscle L-type Ca current. *Proceedings of the International Union of Physiological Sciences* **XVII**, 187 (P2421).

FELDMEYER, D., MELZER, W., POHL, B. & ZÖLLNER, P. (1989*b*). Fast opening kinetics of the slow Ca channel of isolated frog skeletal muscle after conditioning activation. *Journal of Physiology* **415**, 115*P*.

GARCIA, J. & STEFANI, E. (1987). Appropriate conditions to record activation of fast Ca^{2+} channels in frog skeletal muscle (*Rana pipiens*). *Pflügers Archiv* **408**, 646–648.

HENCEK, M., ZACHAROVA, D. & ZACHAR, J. (1988). Fast calcium currents in cut skeletal muscle fibres of the frogs *Rana temporaria* and *Xenopus laevis*. *General Physiology and Biophysics* **7**, 651–656.

HILLE, B. (1984). *Ionic Channels of Excitable Membranes*. Sinauer Associates Inc., Sunderland, MA, USA.

HILLE, B. & CAMPBELL, D. T. (1976). An improved vaseline gap voltage clamp for skeletal muscle fibers. *Journal of General Physiology* **67**, 265–293.

HODGKIN, A. L. & HUXLEY, A. F. (1952). A quantitative description of membrane current and its application to conduction and excitation in nerve. *Journal of Physiology* **117**, 500–544.

HUANG, C. (1988). Intramembrane charge movements in skeletal muscle. *Physiological Reviews* **68**, 1197–1247.

HUI, C. S., MILTON, R. L. & EISENBERG, R. S. (1984). Charge movement in skeletal muscle fibres paralyzed by the calcium-entry blocker D600. *Proceedings of the National Academy of Sciences of the USA* **81**, 2582–2585.

KOVACS, L., RIOS, E. & SCHNEIDER, M. F. (1983). Measurement and modification of free calcium transients in frog skeletal muscle fibres by a metallochromic indicator dye. *Journal of Physiology* **343**, 161–196.

LAMB, G. D. (1986). Components of charge movement in rabbit skeletal muscle: the effect of tetracaine and nifedipine. *Journal of Physiology* **376**, 85–100.

LAMB, G. D. & WALSH, T. (1987). Calcium currents, charge movement and dihydropyridine binding in fast- and slow-twitch muscles of rat and rabbit. *Journal of Physiology* **393**, 595–617.

LÜTTGAU, H. CH., GOTTSCHALK, G. & BERWE, D. (1986). The role of Ca^{2+} in inactivation and paralysis of excitation–contraction coupling in skeletal muscle. *Fortschritte der Zoologie* **33**, 195–203.

LÜTTGAU, H. CH. & SPIECKER, W. (1979). The effect of calcium deprivation upon mechanical and electrophysiological parameters in skeletal muscle fibres of the frog. *Journal of Physiology* **296**, 411–429.

MCDONALD, T. F., CAVALIE, A., TRAUTWEIN, W. & PELZER, D. (1986). Voltage-dependent properties of macroscopic and elementary calcium channel currents in guinea pig ventricular myocytes. *Pflügers Archiv* **406**, 437–448.

MELZER, W., SCHNEIDER, M. F., SIMON, B. J. & SZÜCS, G. (1986). Intramembrane charge movement and calcium release in frog skeletal muscle. *Journal of Physiology* **373**, 481–511.

MIKAMI, A., IMOTO, K., TANABE, T., NIIDOME, T., MORI, Y., TAKESHIMA, H., NARUMIYA, S. & NUMA, S. (1989). Primary structure and functional expression of the cardiac dihydropyridine-sensitive calcium channel. *Nature* **340**, 230–233.

PIZARRO, G., BRUM, G., FILL, M., FITTS, R., RODRIGUEZ, M., URIBE, I. & RIOS, E. (1988). The voltage sensor of skeletal muscle excitation–contraction coupling: a comparison with Ca^{2+} channels. In *The Calcium Channel: Structure, Function and Implications*, ed. MORAD, M., NAYLER, W., KAZDA, S. & SCHRAMM, M., pp. 138–156. Springer–Verlag, Berlin.

RIOS, E. & BRUM, G. (1987). Involvement of dihdropyridine receptors in excitation–contraction coupling in skeletal muscle. *Nature* **325**, 717–720.

SANCHEZ, J. A. & STEFANI, E. (1978). Inward calcium current in twitch muscle fibres of the frog. *Journal of Physiology* **283**, 197–209.

SANCHEZ, J. A. & STEFANI, E. (1983). Kinetic properties of calcium channels of twitch muscle fibres of the frog. *Journal of Physiology* **337**, 1–17.

SCHNEIDER, M. F. & SIMON, B. J. (1988). Inactivation of calcium release from the sarcoplasmic reticulum in frog skeletal muscle. *Journal of Physiology* **405**, 727–745.

SCHWARTZ, L. M., MCCLESKEY, E. W. & ALMERS, W. (1985). Dihydropyridine receptors in muscle are voltage-dependent but most are not functional calcium channels. *Nature* **314**, 747–751.

SIMON, B. J. & SCHNEIDER, M. F. (1988). Time course of activation of calcium release from sarcoplasmic reticulum in skeletal muscle. *Biophysical Journal* **54**, 1159–1163.

TANABE, T., BEAM, K. G., POWELL, J. A. & NUMA, S. (1988). Restoration of excitation–contraction coupling and slow calcium current in dysgenic muscle by dihydropyridine receptor complementary DNA. *Nature* **336**, 134–139.

TANABE, T., TAKESHIMA, H., MIKAMI, A., FLOCKERZI, V., TAKAHASHI, H., KANGAWA, K., KOJIMA, M., MATSUO, H., HIROSE, T. & NUMA, S. (1987). Primary structure of the receptor for calcium channel blockers from skeletal muscle. *Nature* **328**, 313–318.

WHITE, M. M. & BEZANILLA, F. (1985). Activation of squid axon K^+ channels. Ionic and gating current studies. *Journal of General Physiology* **85**, 539–554.